Electronic Supporting Information for:

Synthesis and Properties of a Redox-switchable Calix[6]arene-based Molecular Lasso

Guido Orlandini, Lorenzo Casimiro, Margherita Bazzoni, Beatrice Cogliati, Alberto Credi, Marco Lucarini, Serena Silvi, Arturo Arduini, and Andrea Secchi

Contents:

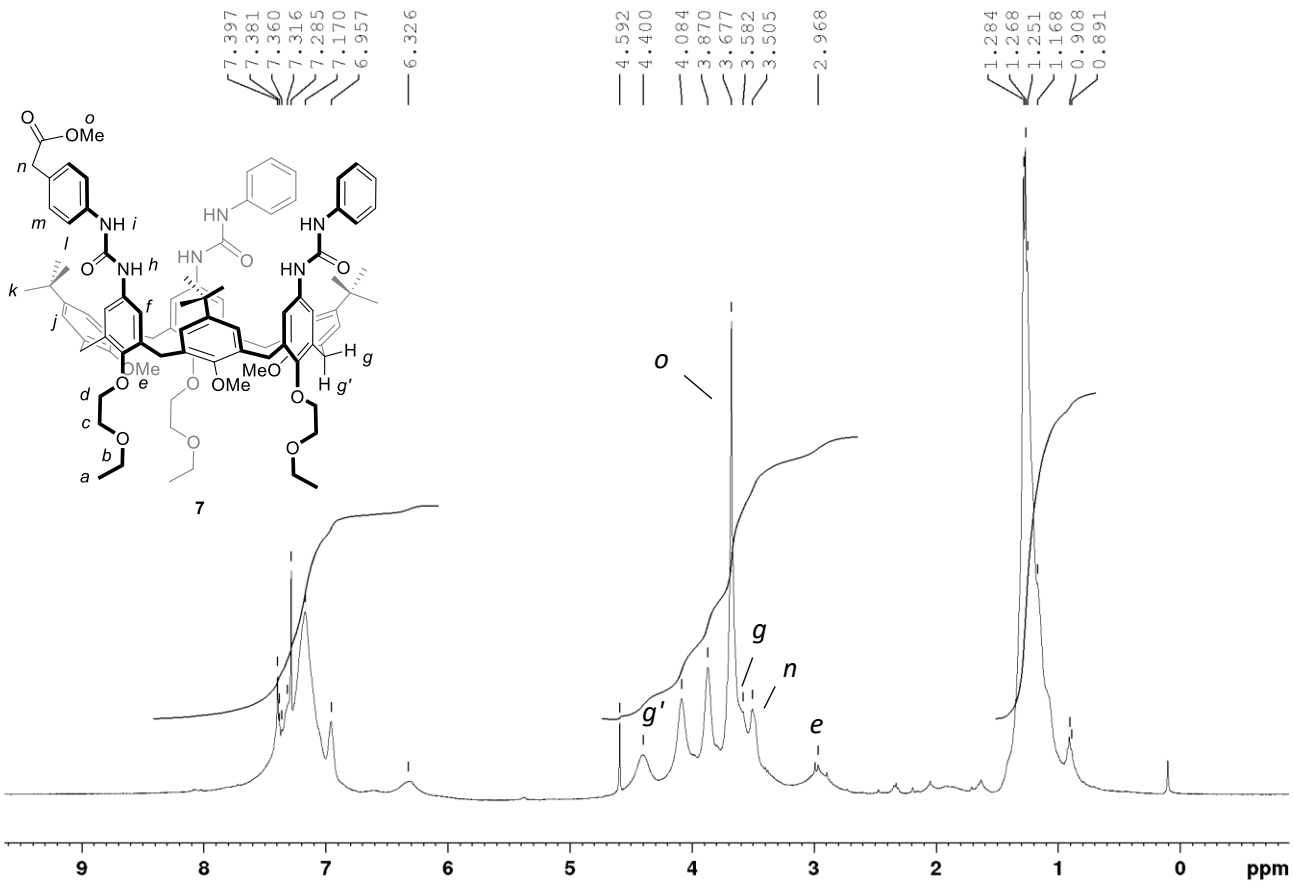

Figure S1. ^{1}H NMR (400 MHz, $CDCl_3$) spectrum of calix[6]arene **7**.

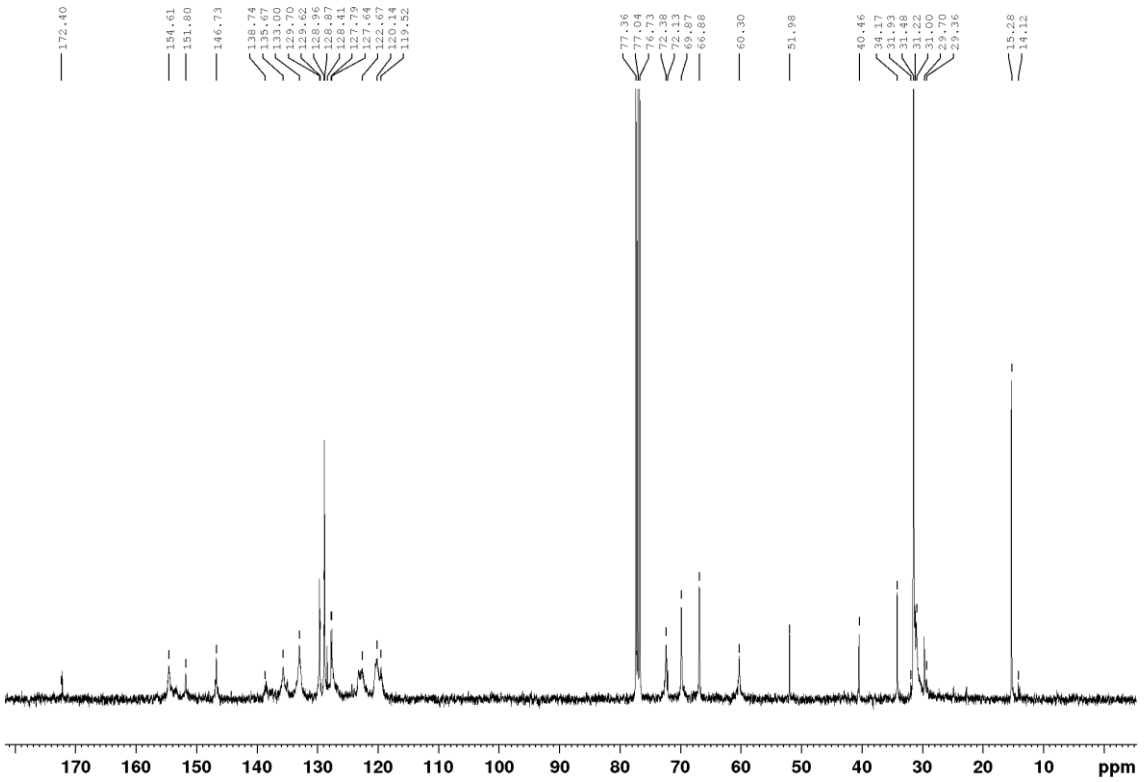

Figure S2. ^{13}C NMR (100 MHz, $CDCl_3$) spectrum of calix[6]arene **7**.

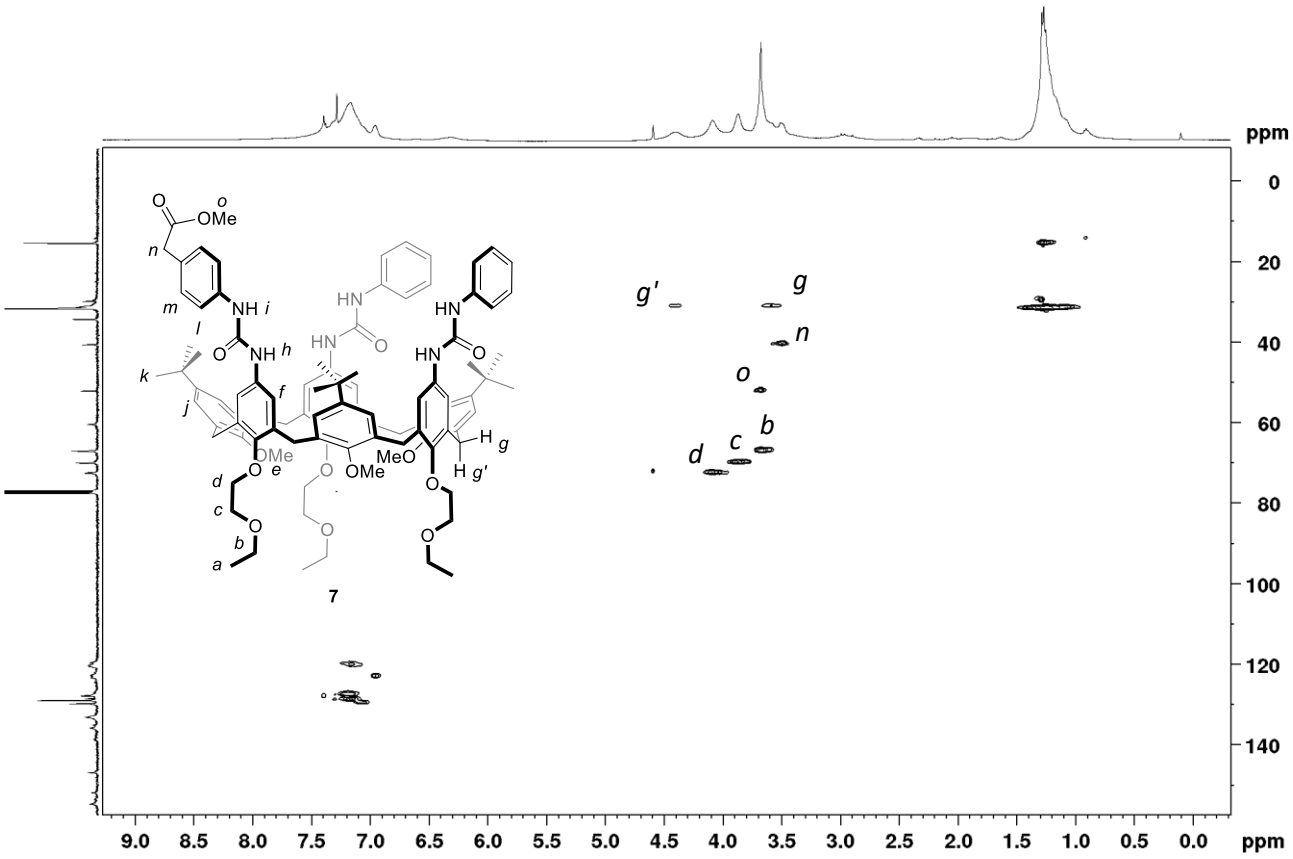

Figure S3. 2D HSQC (400 MHz, $CDCl_3$) spectrum of calix[6]arene **7**.

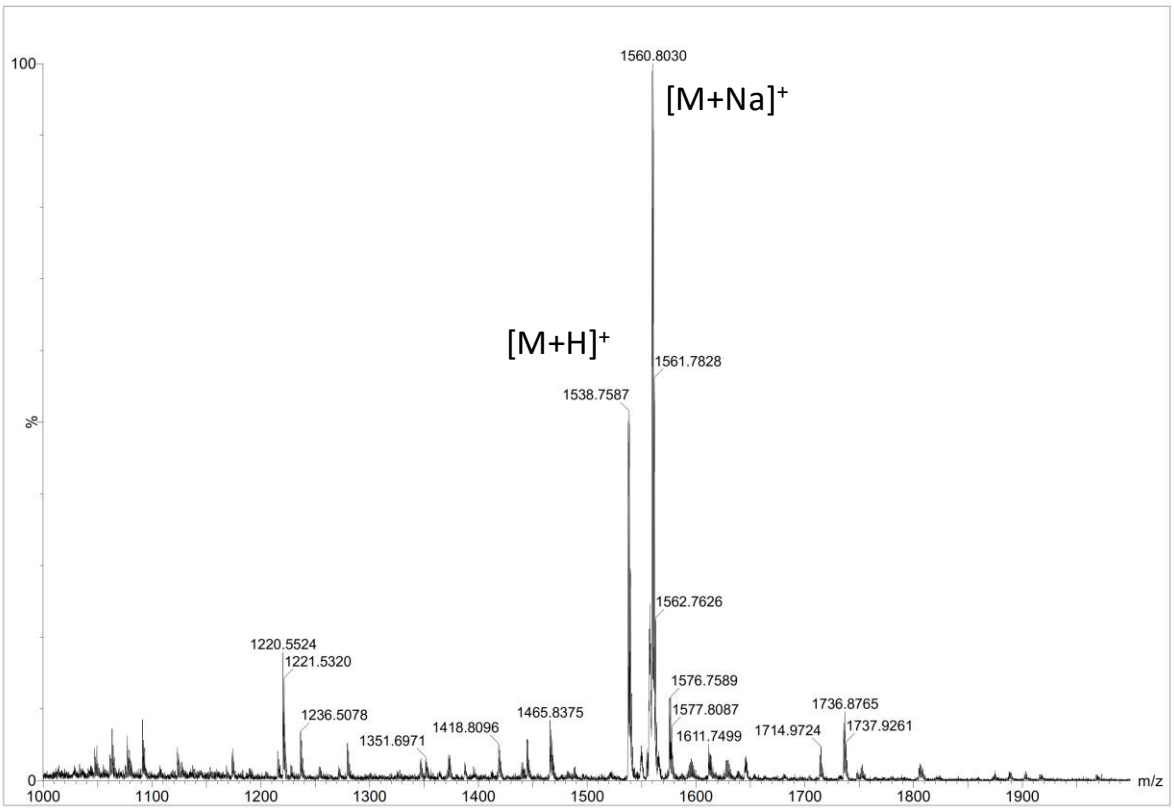

Figure S4. ESI-MS (+) spectrum of calix[6]arene **7**.

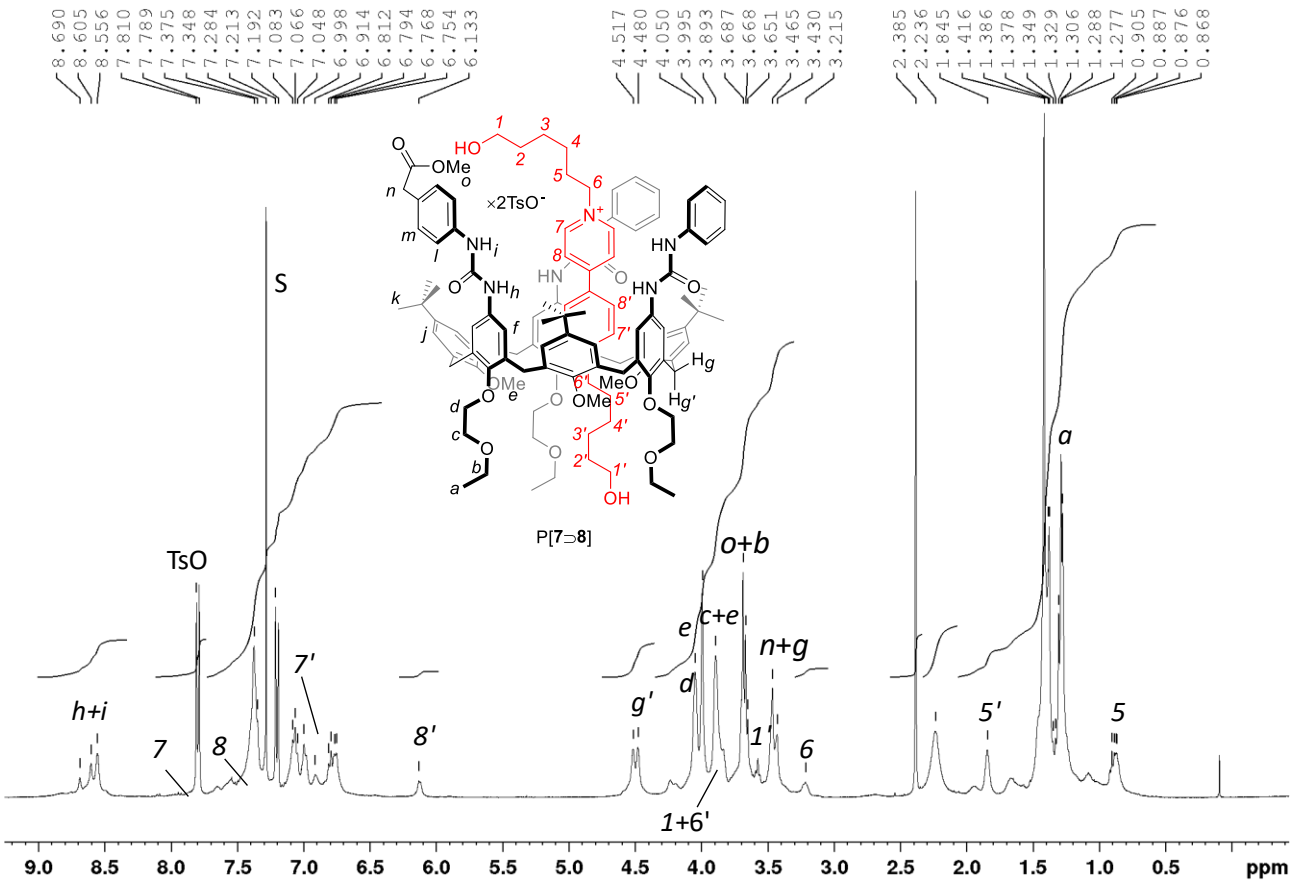

Figure S5. ^{1}H NMR (400 MHz, $CDCl_3$) spectrum of pseudorotaxane P[**7**⊃**8**].

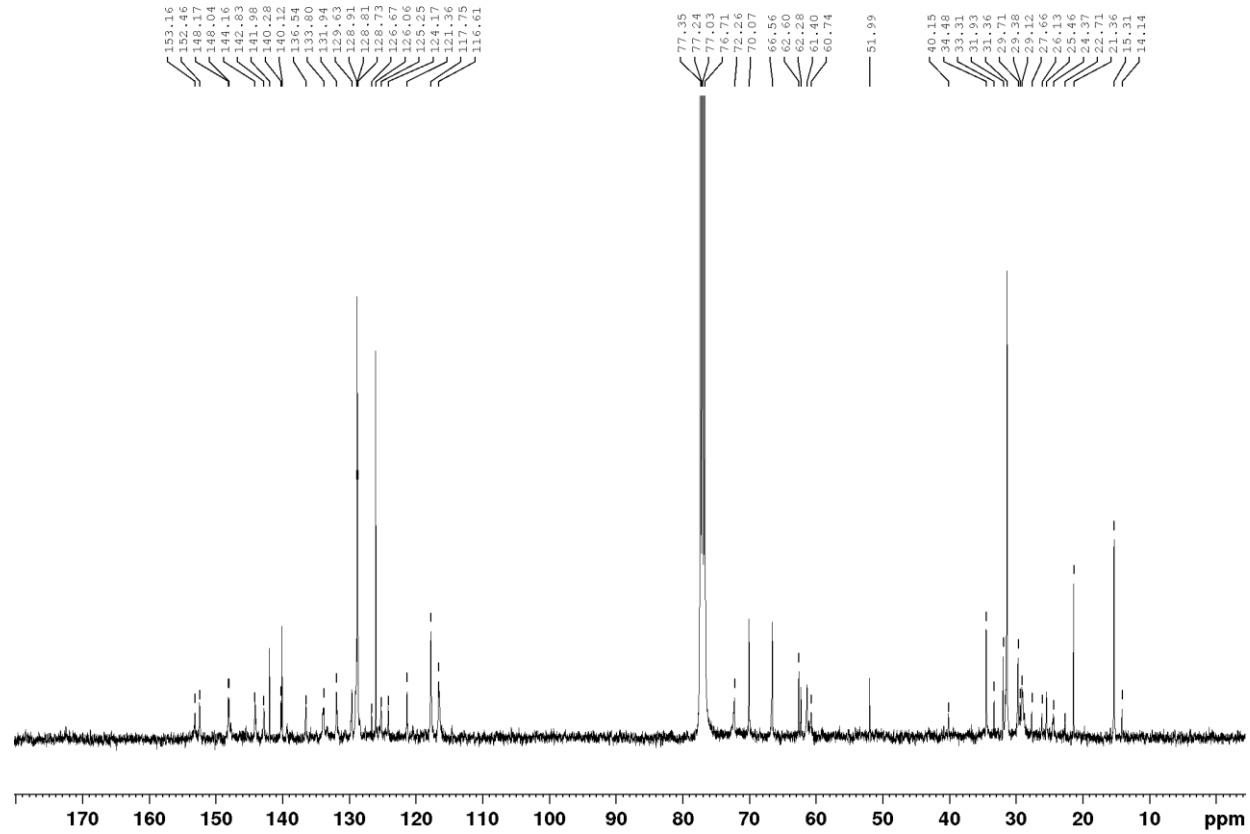

Figure S6. ^{13}C NMR (100 MHz, $CDCl_3$) spectrum of pseudorotaxane P[**7**⊃**8**].

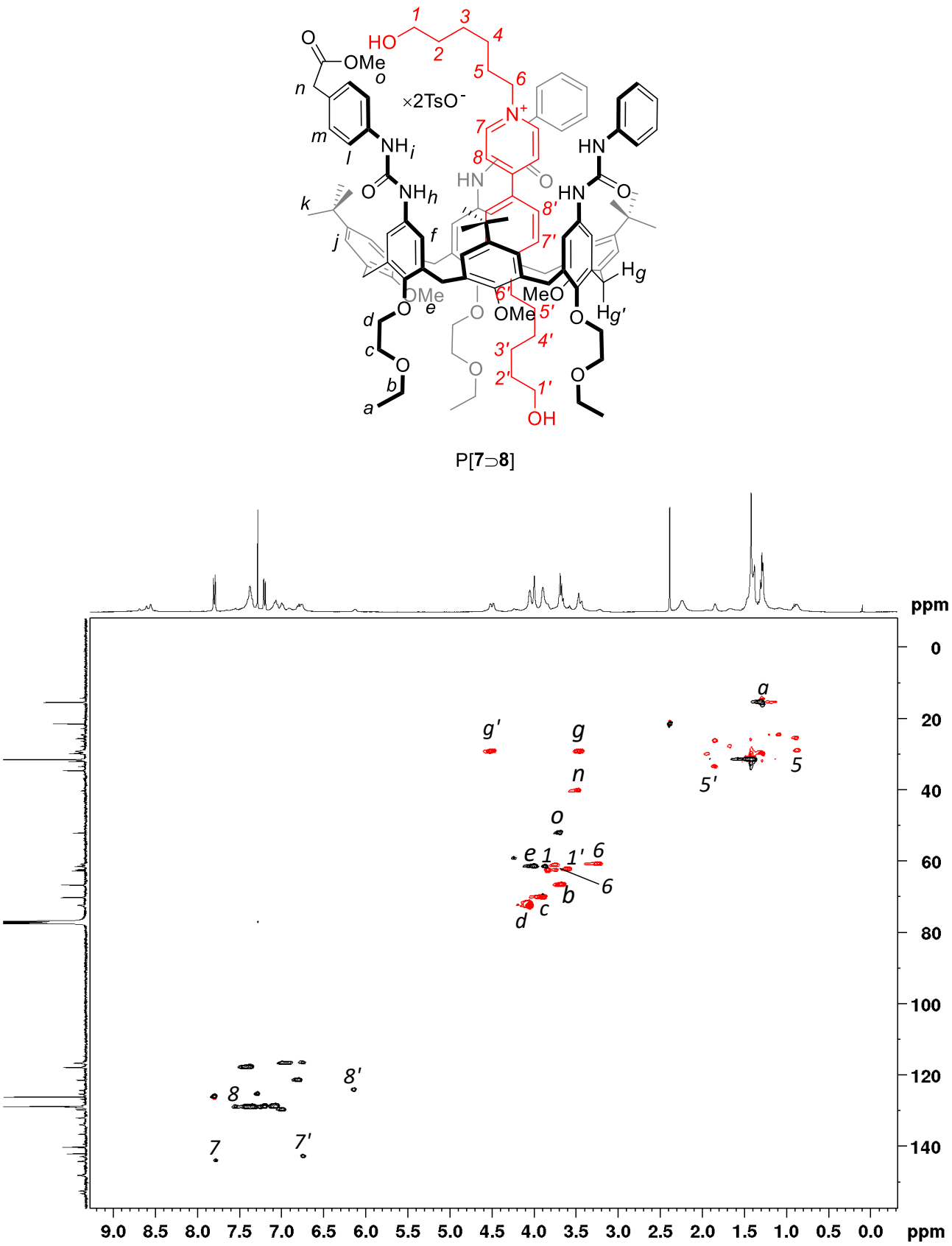

Figure S7. 2D edited HSQC spectrum (400 MHz, $CDCl_3$) of pseudorotaxane P[**7**⊃**8**] (cross-peaks correlating secondary carbons in red contours). The most representative assignments have been indicated with letters according to the above sketch.

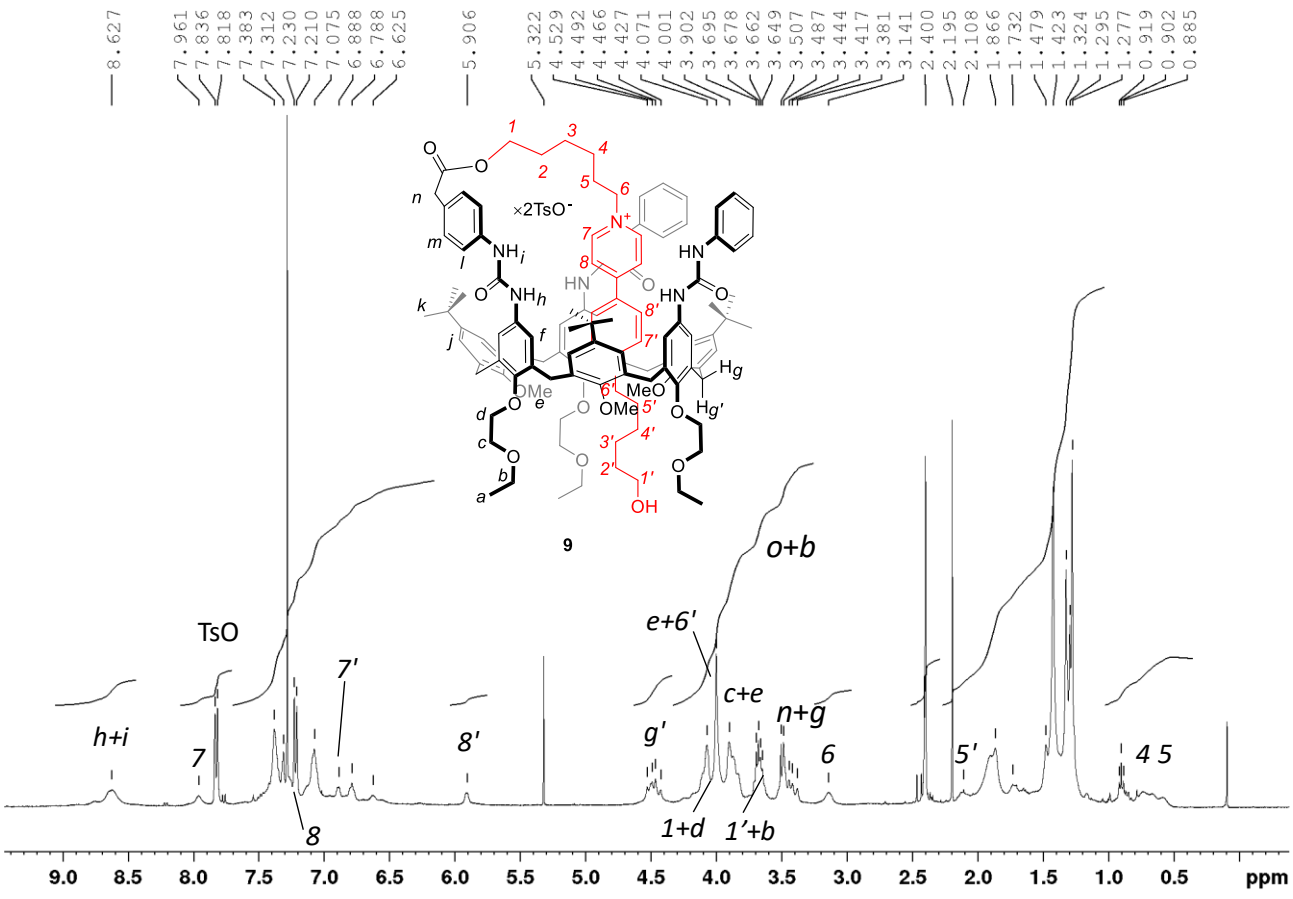

Figure S8. ^{1}H NMR (400 MHz, $CDCl_3$) spectrum of calix[6]arene **9**.

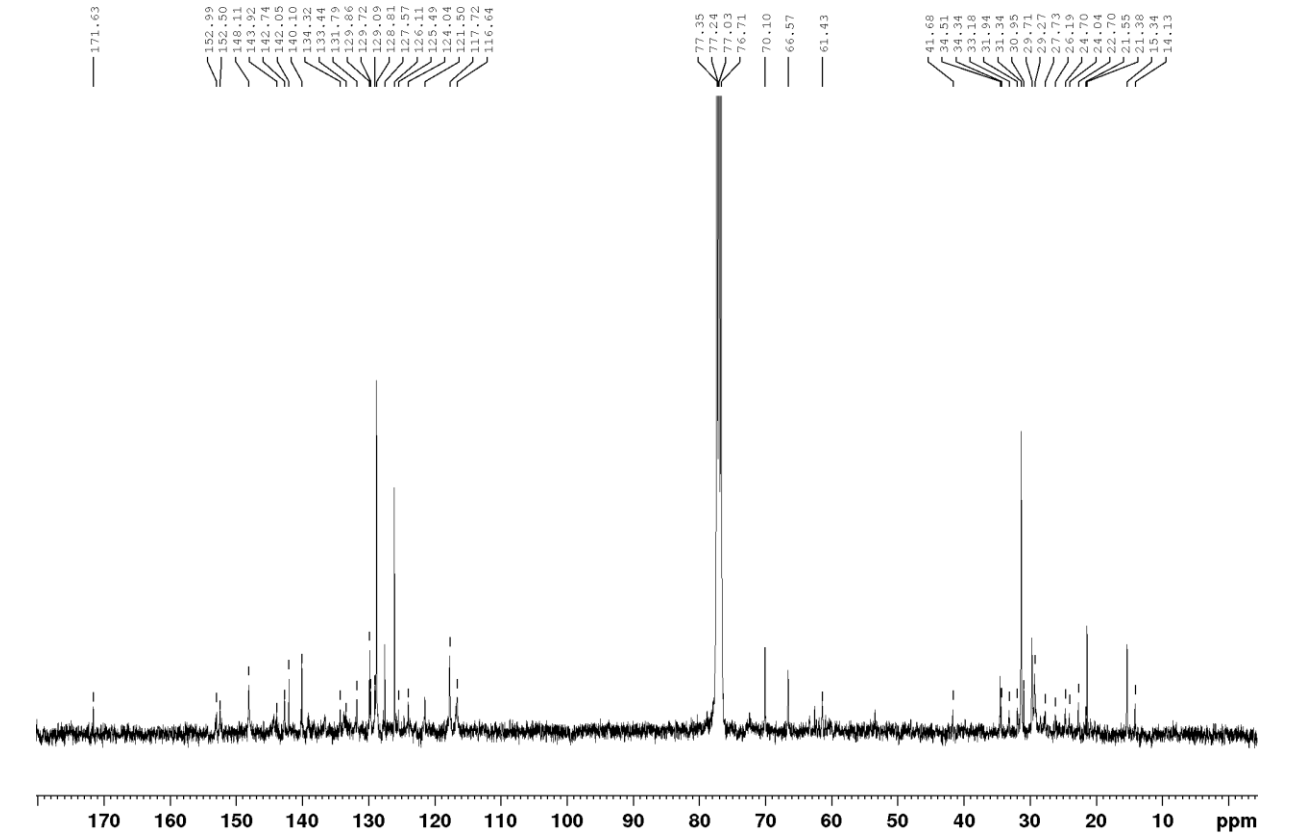

Figure S9. ^{13}C NMR (100 MHz, $CDCl_3$) spectrum of calix[6]arene **9**.

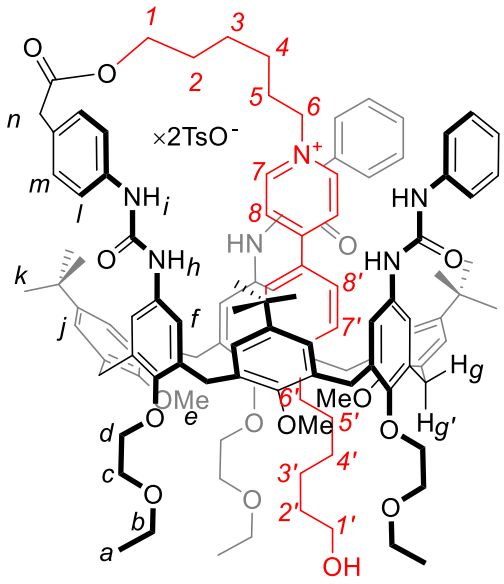

9

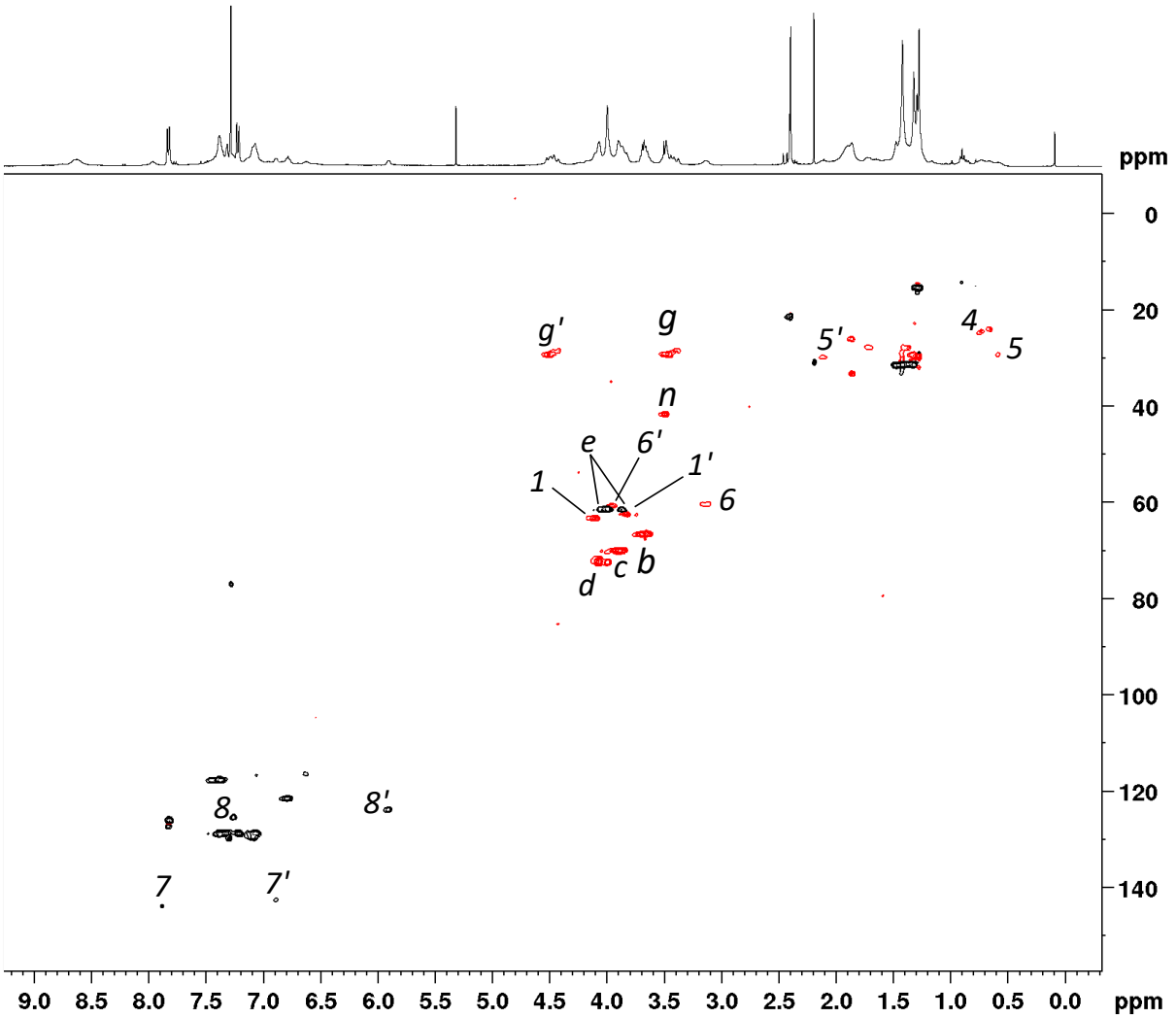

Figure S10. 2D edited HSQC spectrum (400 MHz, $CDCl_3$) of pseudorotaxane **9** (cross-peaks correlating secondary carbons in red contours). The most representative assignments have been indicated with letters according to the above sketch.

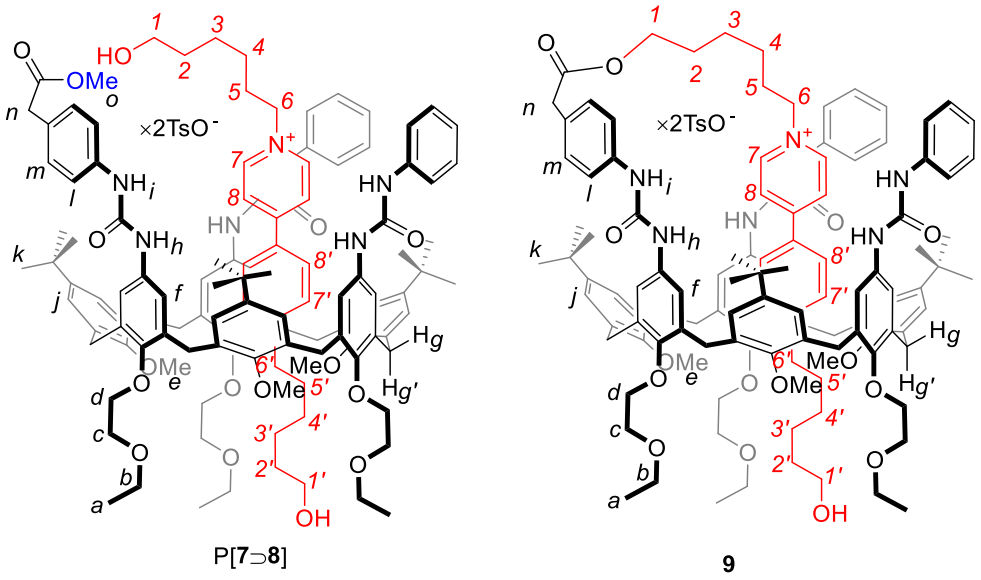

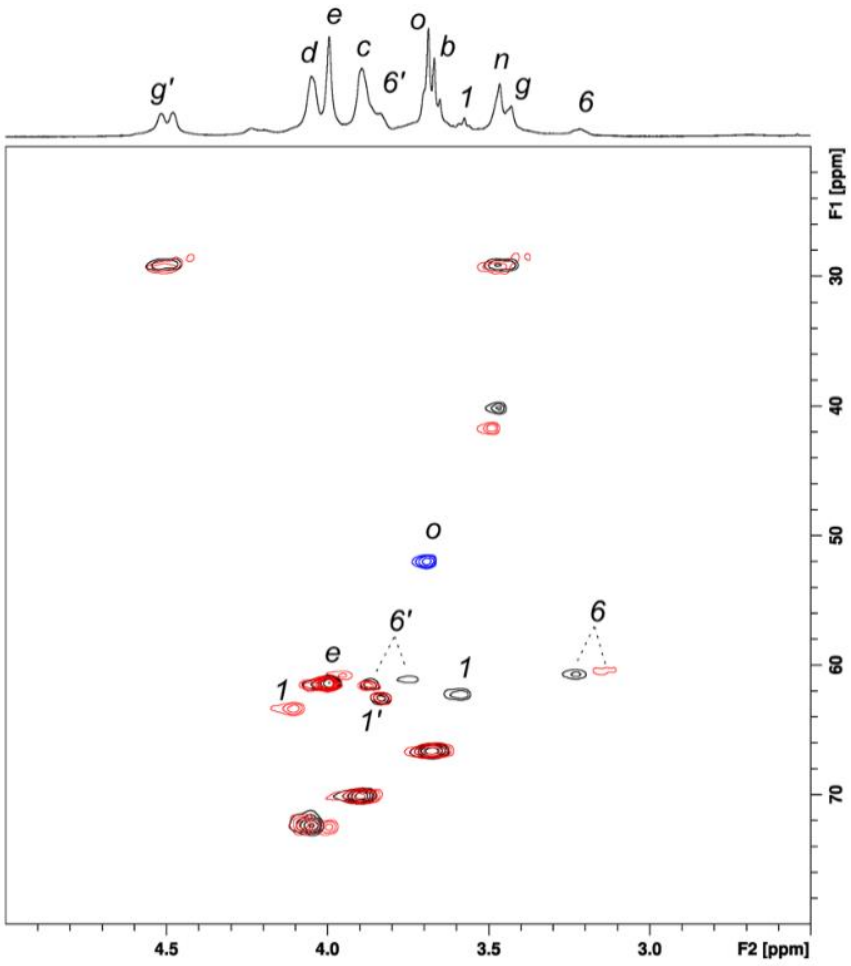

Figure S11. Superimposed ^{1}H-^{13}C 2D HSQC spectra (expanded region) in $CDCl_3$ of pseudorotaxane P[**7**⊃**8**] (black contour lines) and of self-threaded calix[6]arene **9** (red contour lines). The linkage between the axial component and the calix[6]arene wheel was confirmed by the disappearing of the cross-peak relative to the methylester group (*o*) at (F_2,F_1) = 3.69, 52.0 ppm and by the downfield shift of the cross-peak relative to the methylene group (*1*) from (F_2,F_1) = 3.58, 62.1 ppm (black contour lines) to (F_2,F_1) = 4.16, 63.2 ppm (red contour lines). The F_2 projection is relative to pseudorotaxane P[**7**⊃**8**]. For the labels, see the scheme above the spectrum.

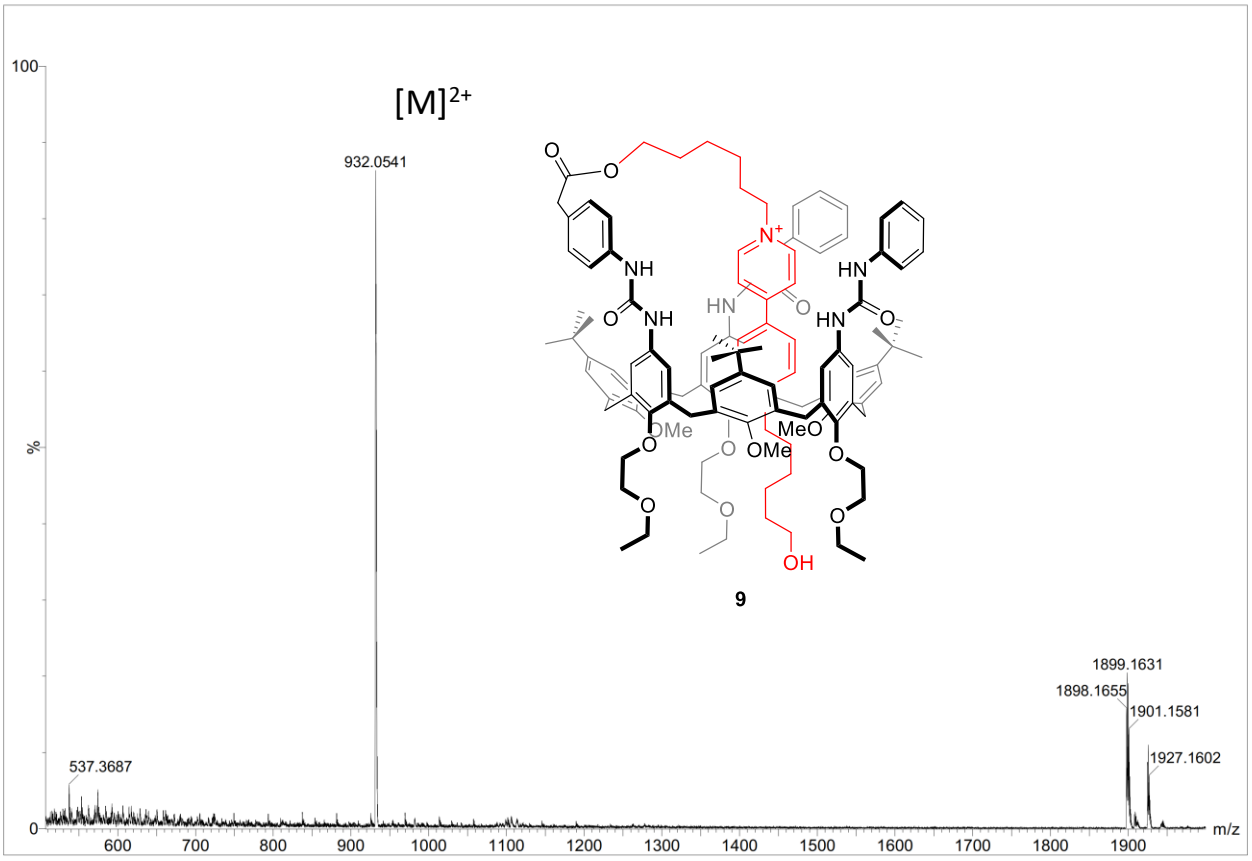

Figure S12. ESI-MS (+) spectrum of calix[6]arene **9**

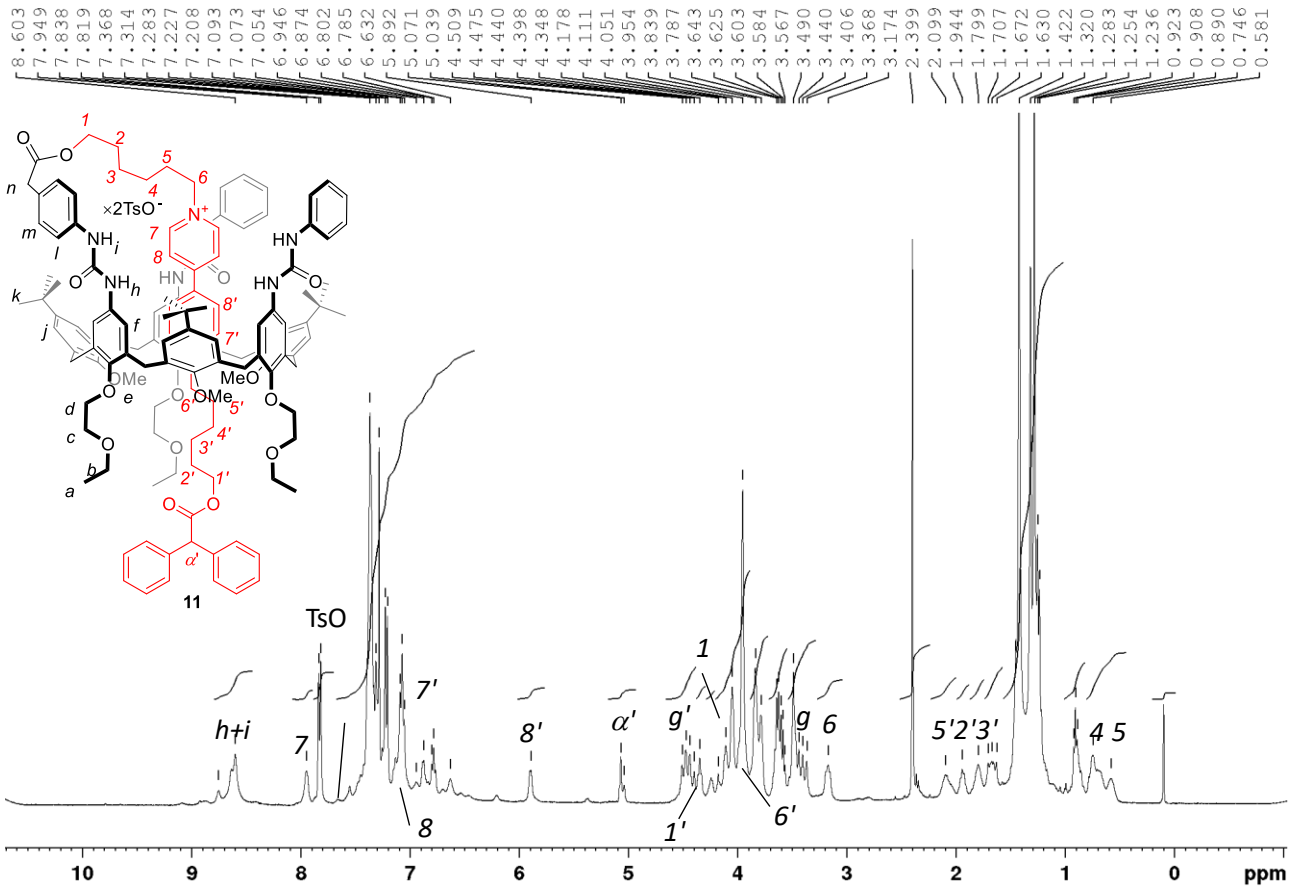

Figure S13. ^{1}H NMR (400 MHz, $CDCl_3$) spectrum of calix[6]arene **11**.

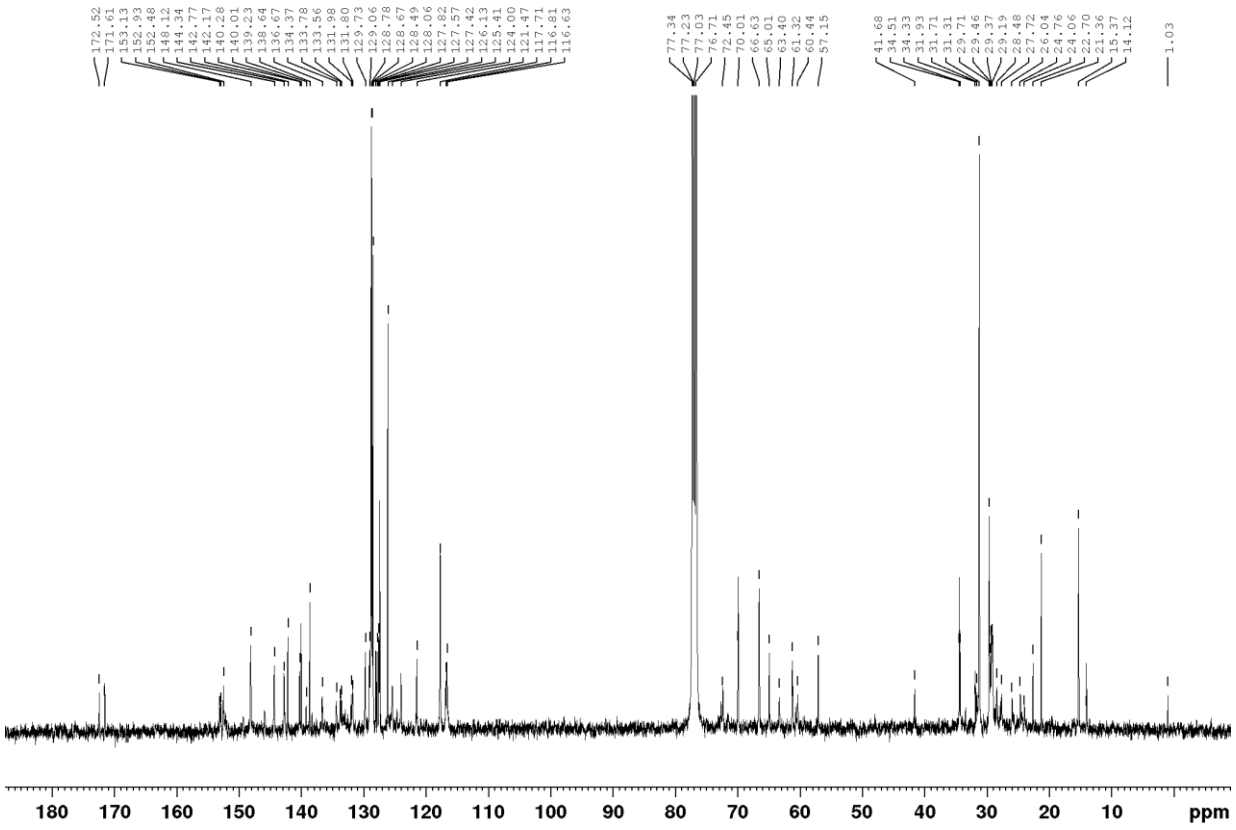

Figure S14. ^{13}C NMR (100 MHz, $CDCl_3$) spectrum of calix[6]arene **11**.

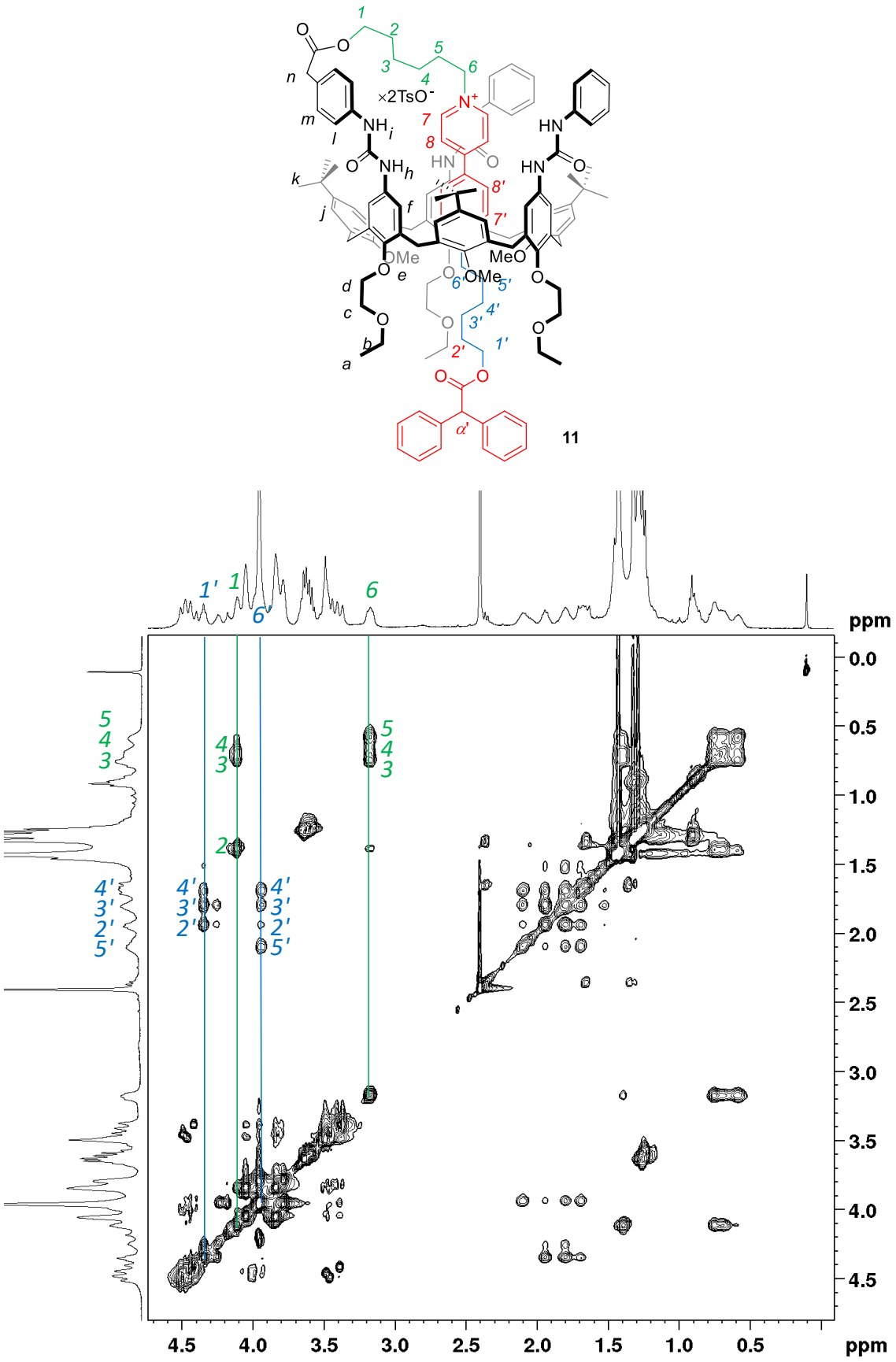

Figure S15. Expanded region of the 2D TOCSY (400 MHz, $CDCl_3$) spectrum of calix[6]arene **11** (mixing time = 0.08 s): the green and blue lines denote the correlations of the two alkyl chains appended to the bispyridinium core.

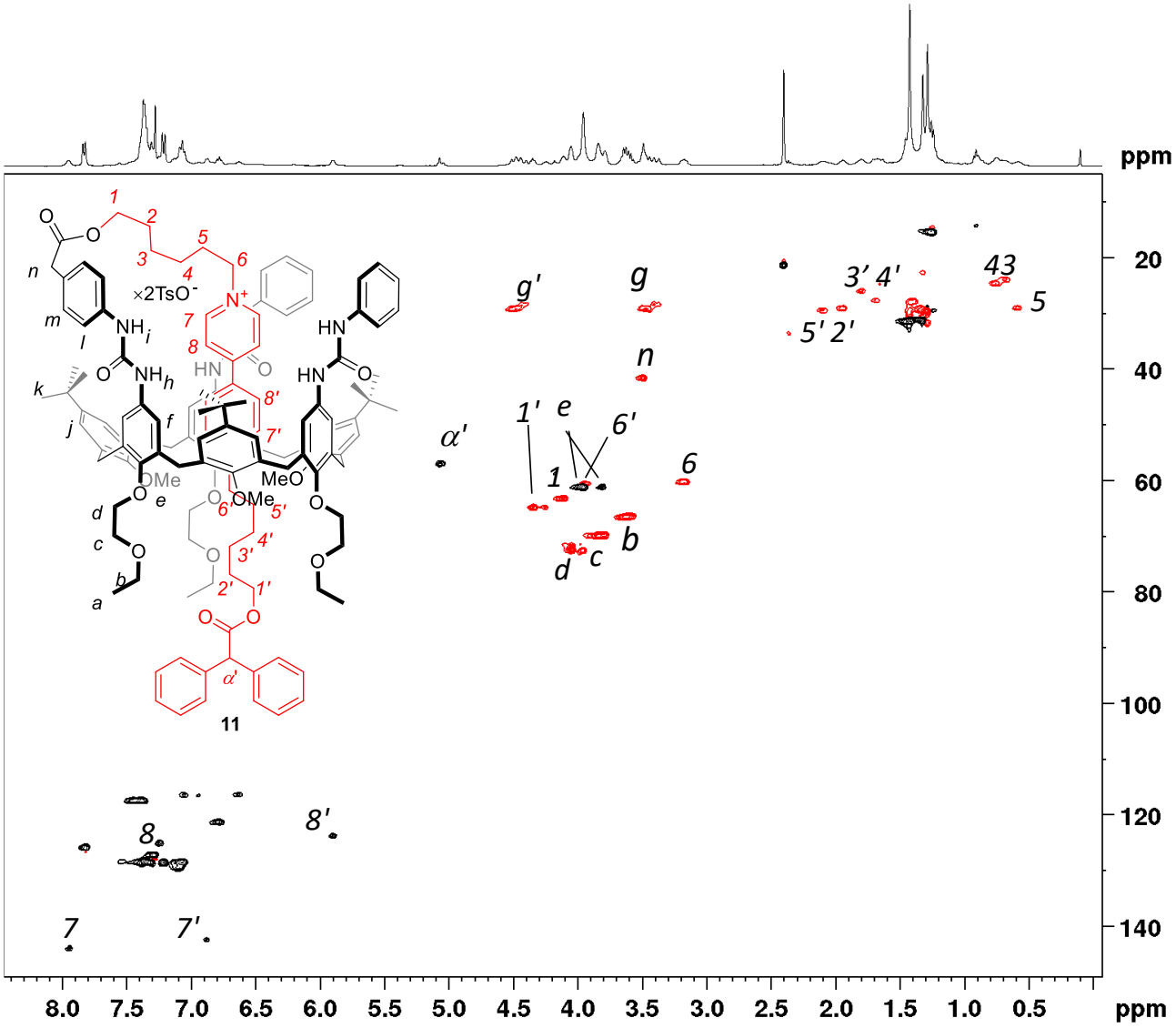

Figure S16. 2D ed.HSQC spectrum (400 MHz, $CDCl_3$) of calix[6]arene **11** (secondary carbons in red).

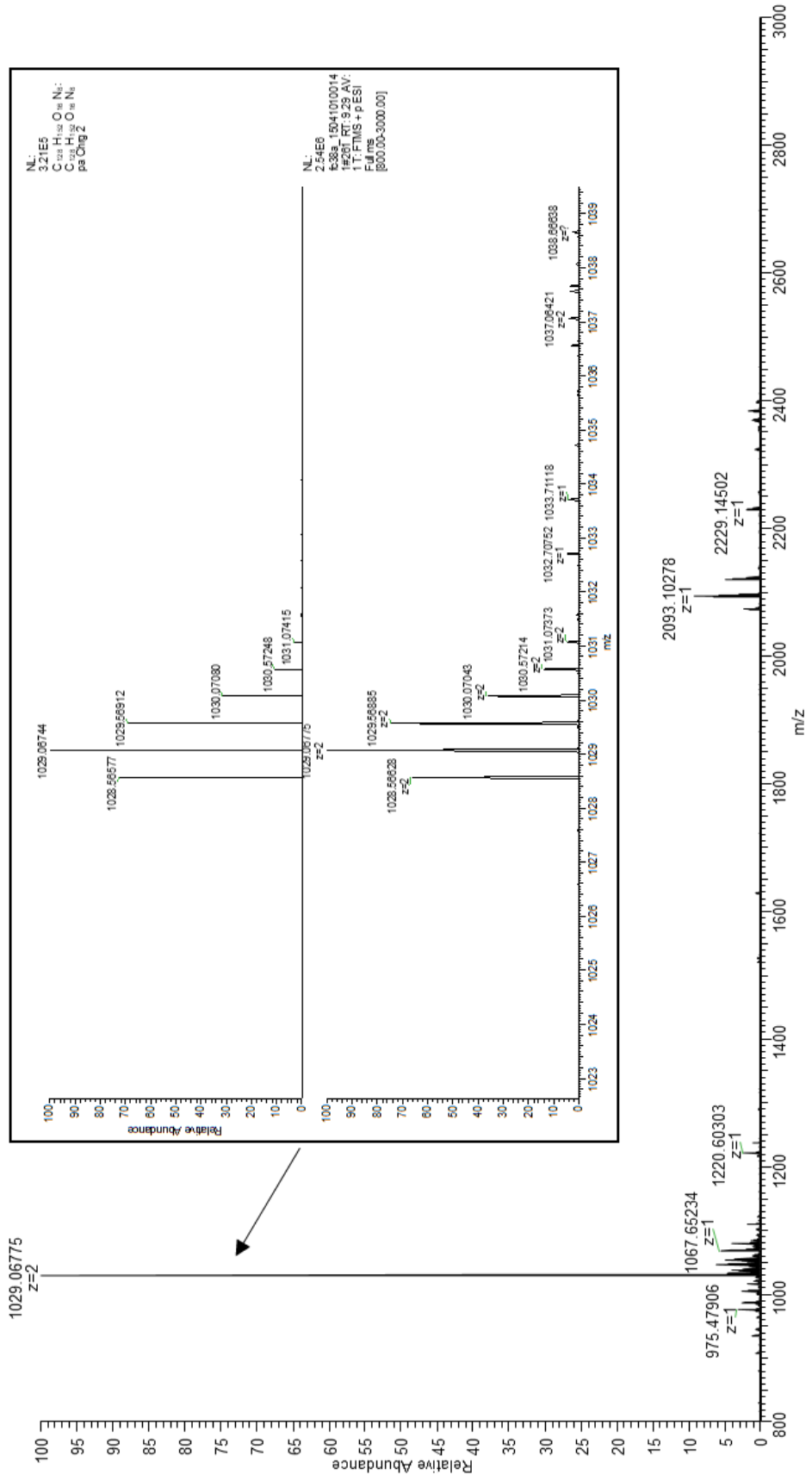

Figure S17. ESI-MS (+) (Orbitrap LQ) spectrum of calix[6]arene **11**. The inset shows the real and the simulated spectra of the doubly charged specie indicated by the arrow.

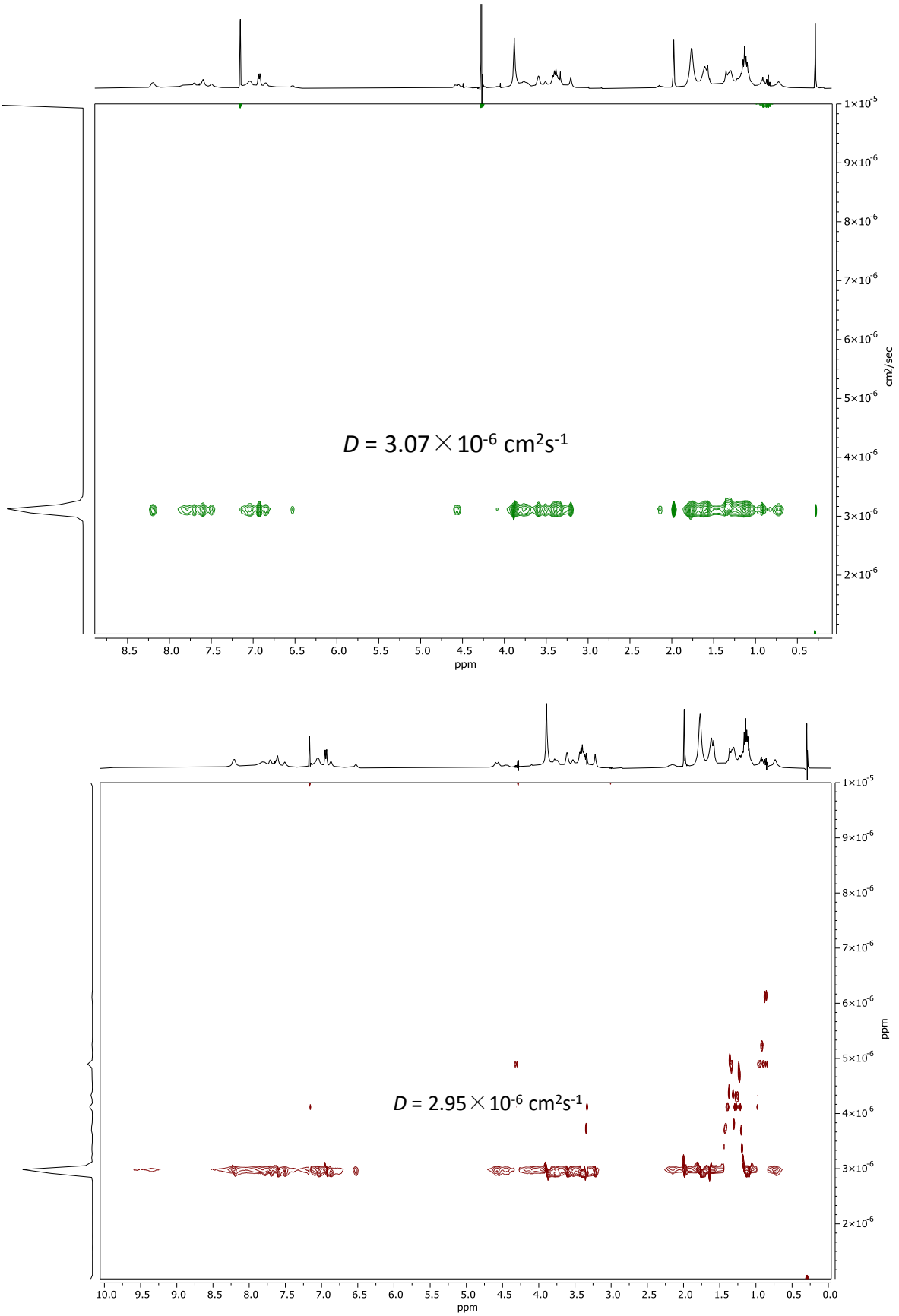

Figure S18. DOSY (400 MHz) spectra of a 7 (top) and 12 mM (down) solution in C_6D_6 of calix[6]arene **9**. The measured diffusion coefficients are indicated on the spectra.

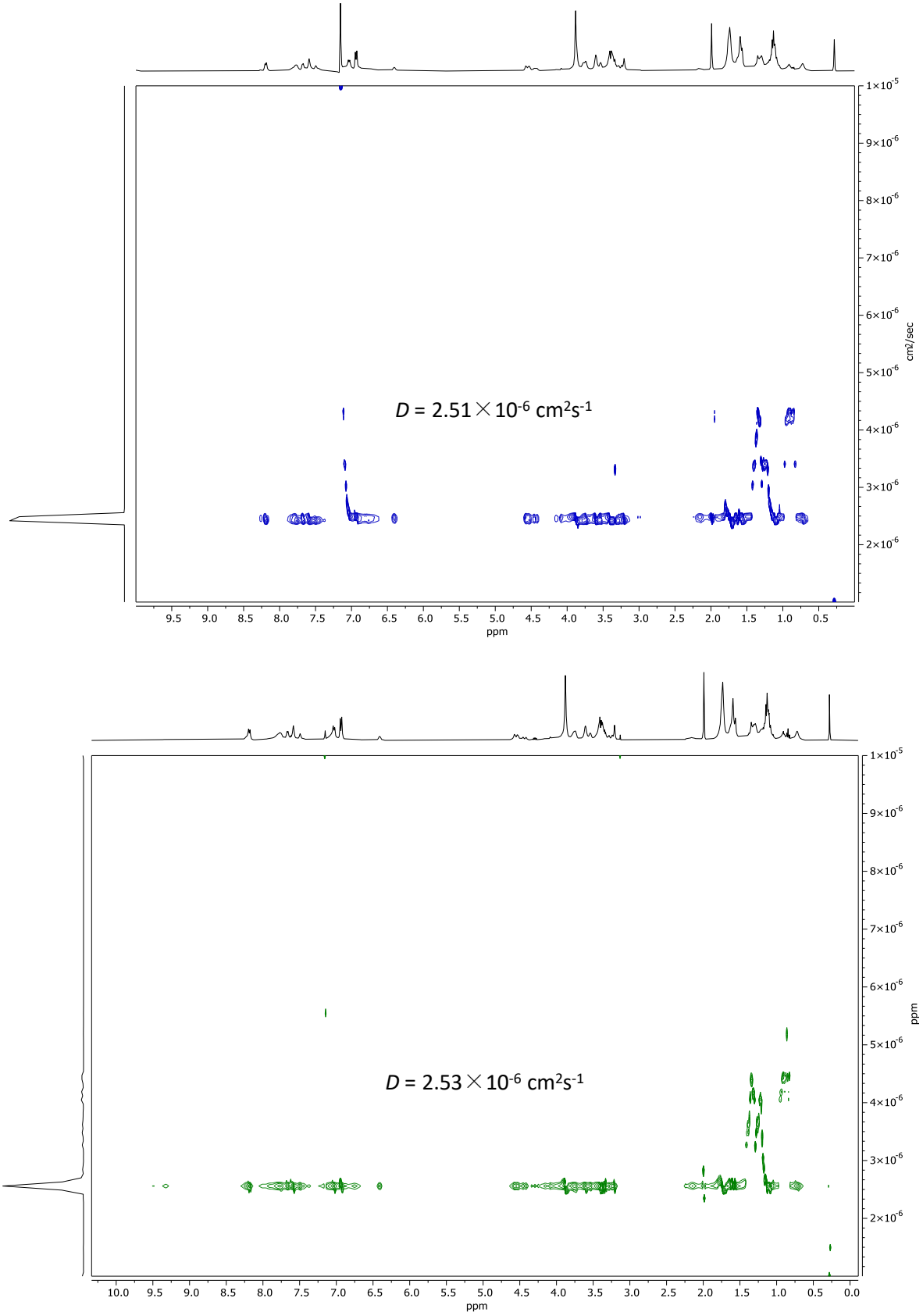

Figure S19. DOSY (400 MHz) spectra of a 22 mM (top) and 30 mM (down) solution in C_6D_6 of calix[6]arene **9**. The measured diffusion coefficients are indicated on the spectra.

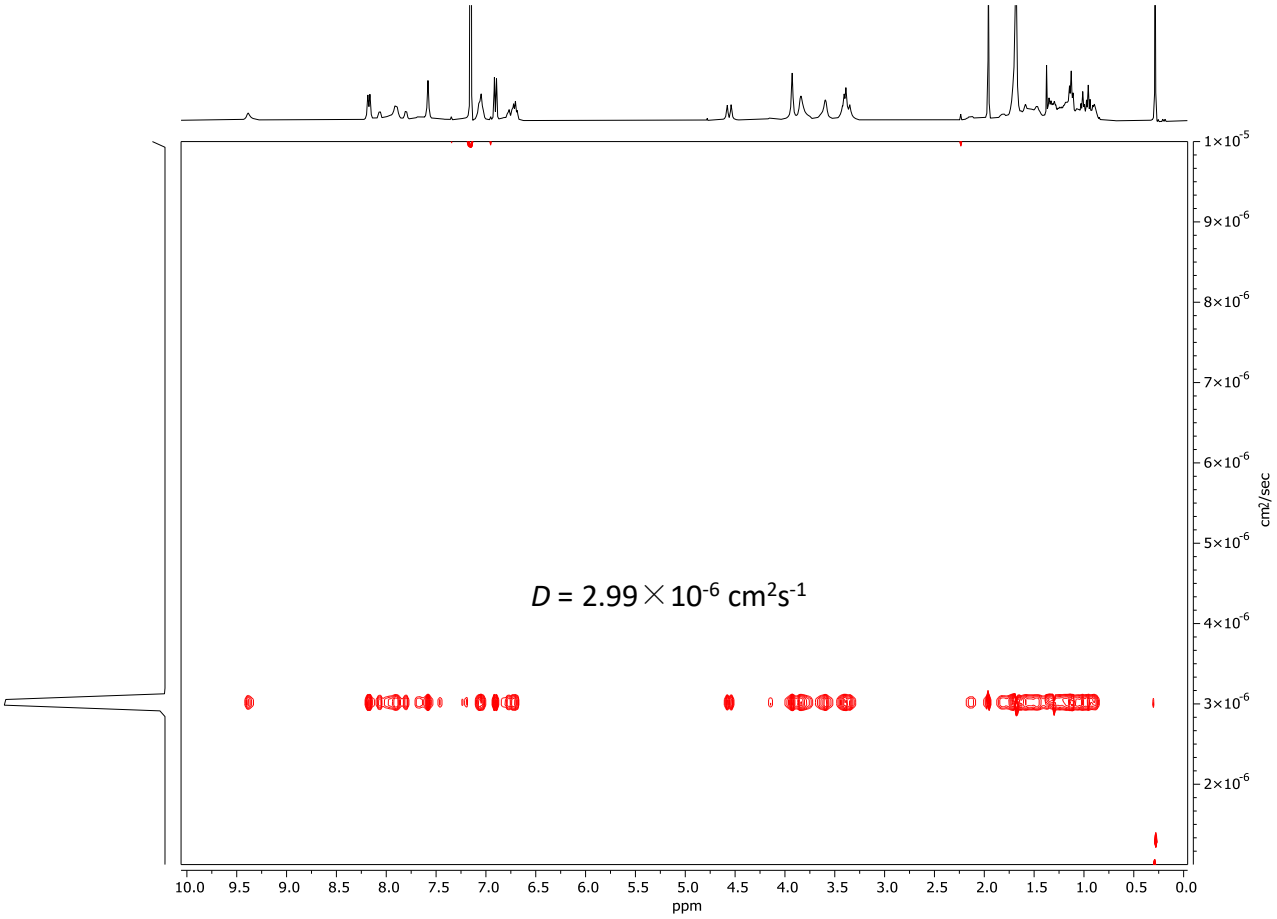

Figure S20. DOSY (400 MHz) spectra of a 7 mM solution in C_6D_6 of pseudorotaxane P[**1**⊃**10**]. The measured diffusion coefficients are indicated on the spectra.

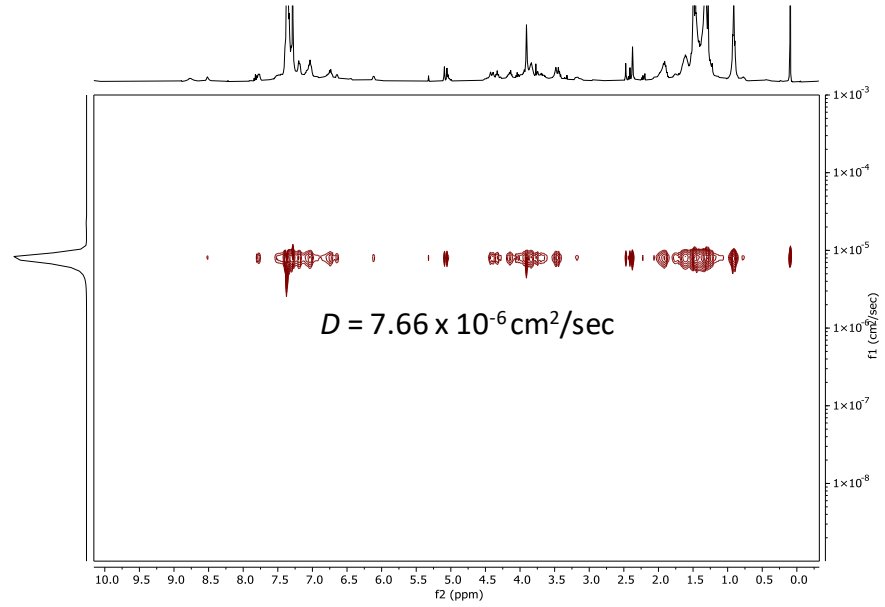

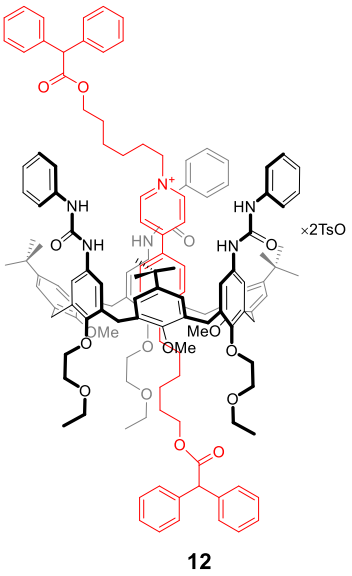

12

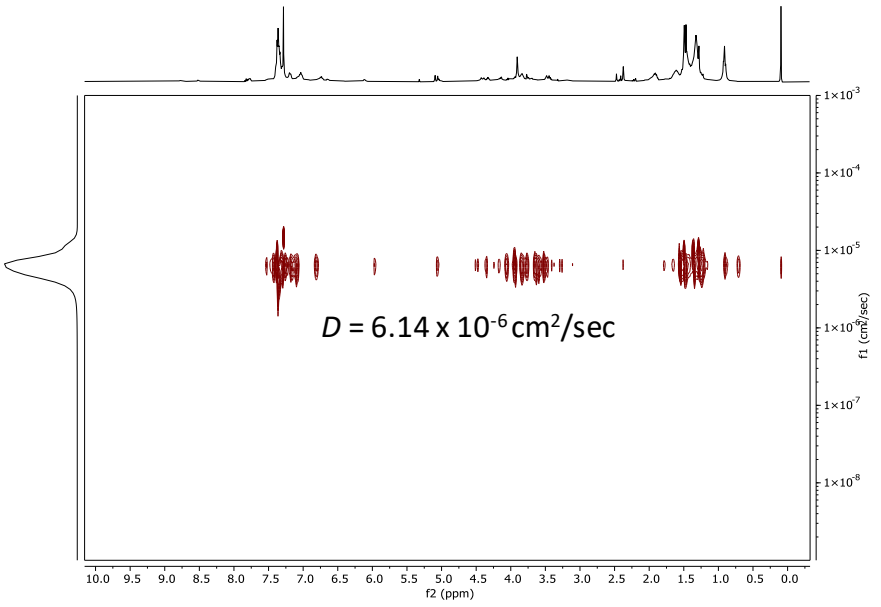

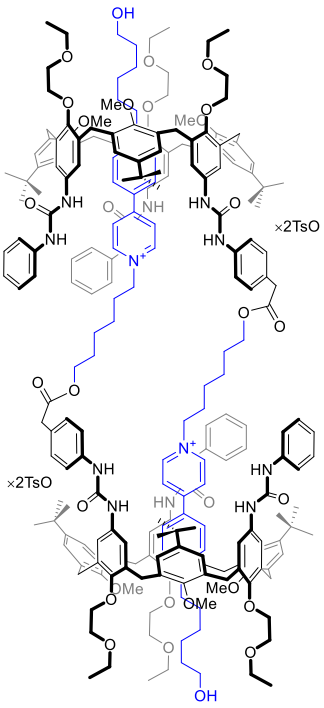

[*c2*]**9**

Figure S21. DOSY (400 MHz) spectra of a 50 mM solution in C_6D_6 of calix[6]arene-based [2]rotaxane **12** (top), and of calix[6]arene **9** (bottom). The measured diffusion coefficients are indicated on the spectra.

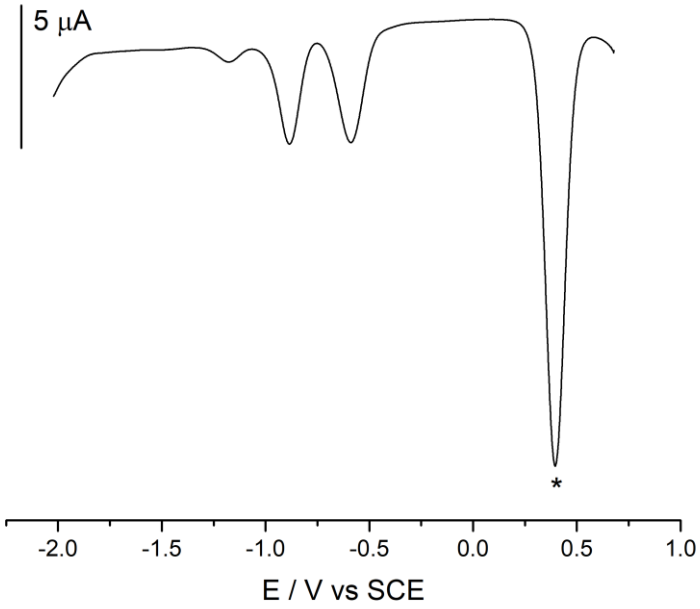

Figure S22. Differential pulse voltammetry of a 1.8 × 10^{-4} M solution of [1]pseudorotaxane **9** in CH_3CN in presence of 100 equivalents of $TBAPF_6$. The asterisk indicates the redox process of $Fc/Fc^{\cdot+}$.

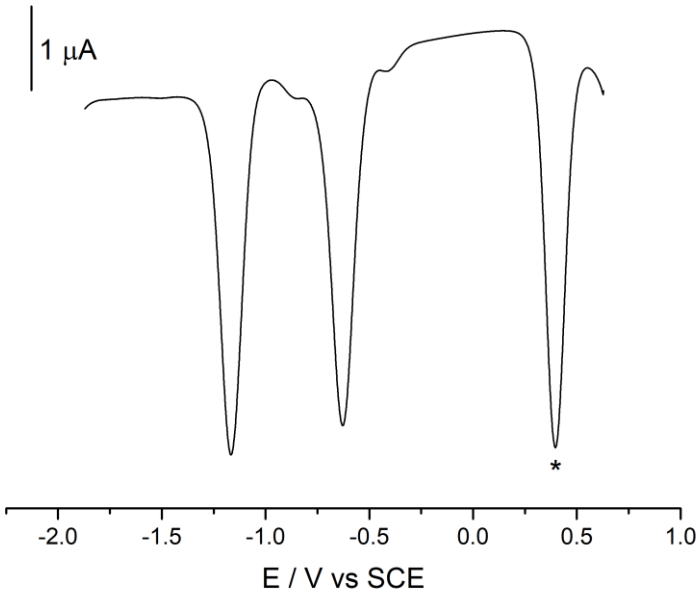

Figure S23. Differential pulse voltammetry of a 1.5 × 10^{-4} M solution of [1]rotaxane **11** in CH_3CN in presence of 100 equivalents of $TBAPF_6$. The asterisk indicates the redox process of $Fc/Fc^{\cdot+}$.

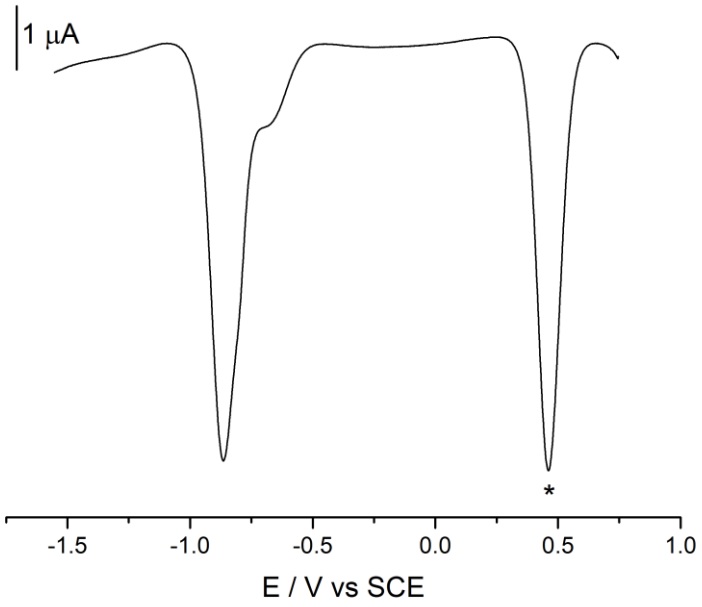

Figure S24. Differential pulse voltammetry of a 2.4 × 10^{-4} M solution of [1]pseudorotaxane **9** in CH_2Cl_2 in presence of 100 equivalents of $TBAPF_6$. The asterisk indicates the redox process of $Fc/Fc^{\cdot+}$.

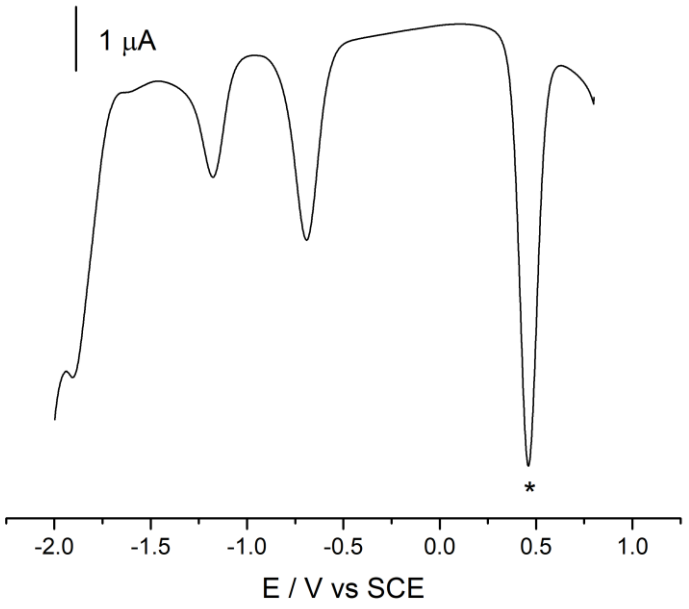

Figure S25. Differential pulse voltammetry of a 1.4 × 10^{-4} M solution of [1]rotaxane **11** in CH_2Cl_2 in presence of 100 equivalents of $TBAPF_6$. The asterisk indicates the redox process of $Fc/Fc^{\cdot+}$.

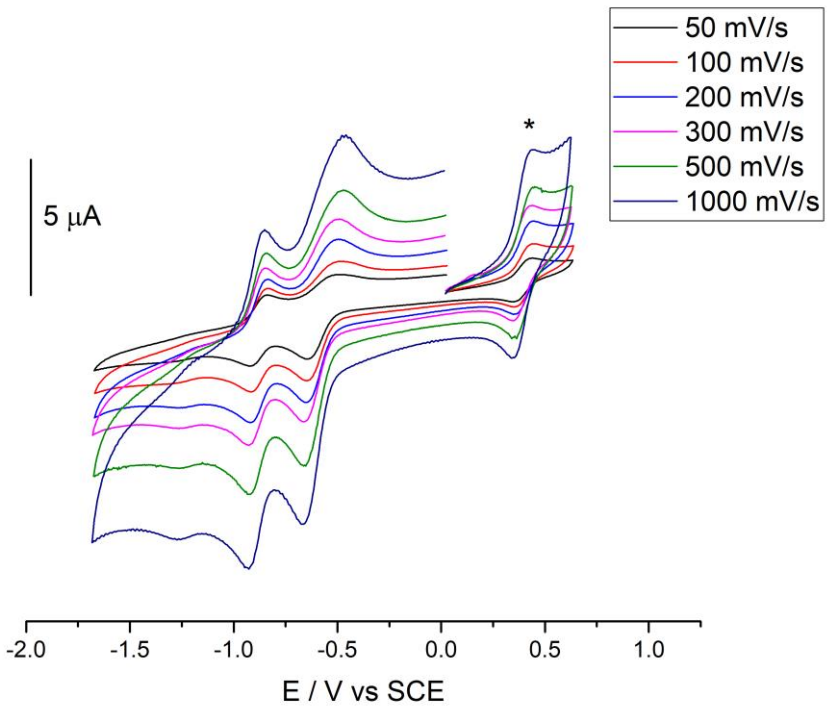

Figure S26. Cyclic voltammograms at different scan rates of a 1.6×10^{-4} M solution of [1]pseudorotaxane **9** in CH_3CN in presence of 100 equivalents of $TBAPF_6$. The asterisk indicates the redox wave of ferrocene used as an internal standard.

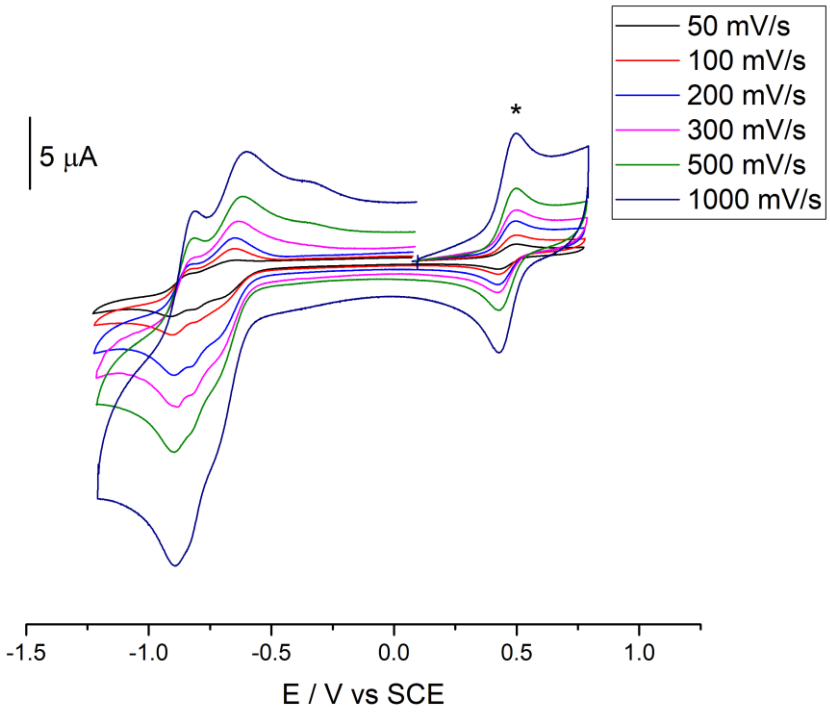

Figure S27. Cyclic voltammograms at different scan rates of a 1.8×10^{-4} M solution of [1]pseudorotaxane **9** in CH_2Cl_2 in presence of 100 equivalents of $TBAPF_6$. The asterisk indicates the redox wave of ferrocene used as an internal standard. The weak bump on the cathodic wave at about -0.8 V is assigned to traces of oxygen.

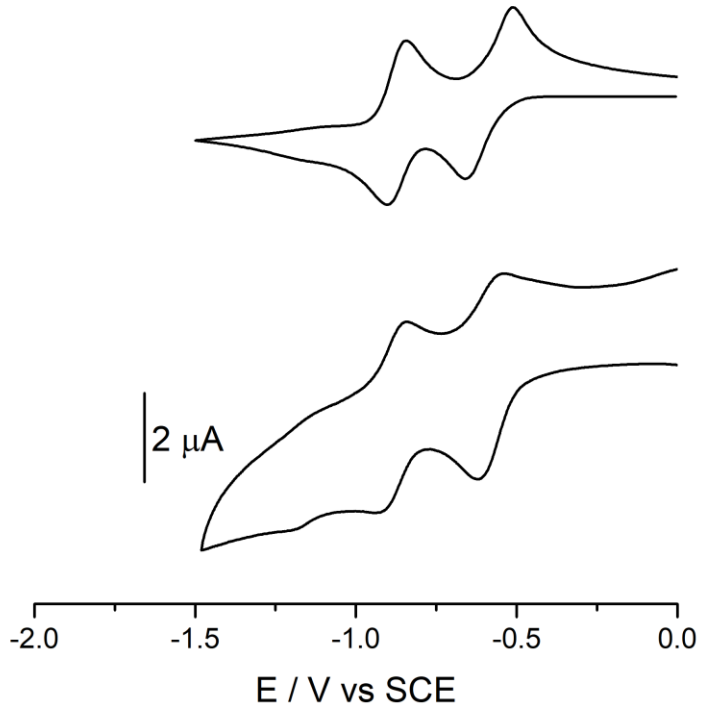

Figure S28. Simulated (top) and experimental (bottom, 1.5 × 10^{-4} M, scan rate 100 mV/s) cyclic voltammograms of [1]pseudorotaxane **9** in CH_3CN. Digital simulations of the experimental CVs were obtained on the basis of the mechanism illustrated in Scheme 2 (main text) by using the software package DigiSim 3.05.[1] The voltammetric curves were simulated with the mechanism reported in Scheme 2, by fixing the values of the reduction potentials of the free (E_1^f and E_2^f) and complexed (E_1^c and E_2^c) species to the ones of **10** and **11**, respectively. A value of 1 cm s^{-1}, representative of a reversible process under our conditions,[2] was employed in the simulation for the free species; the value of the heterogeneous electron-transfer rate constant was estimated from the variation in the peak-to-peak separation as a function of the scan rate by using the Nicholson method[3] for the complexed species. The charge-transfer coefficients were taken as 0.5 in all cases. The quality of the simulation was judged by comparing the values of the peak potentials with the experimental data.

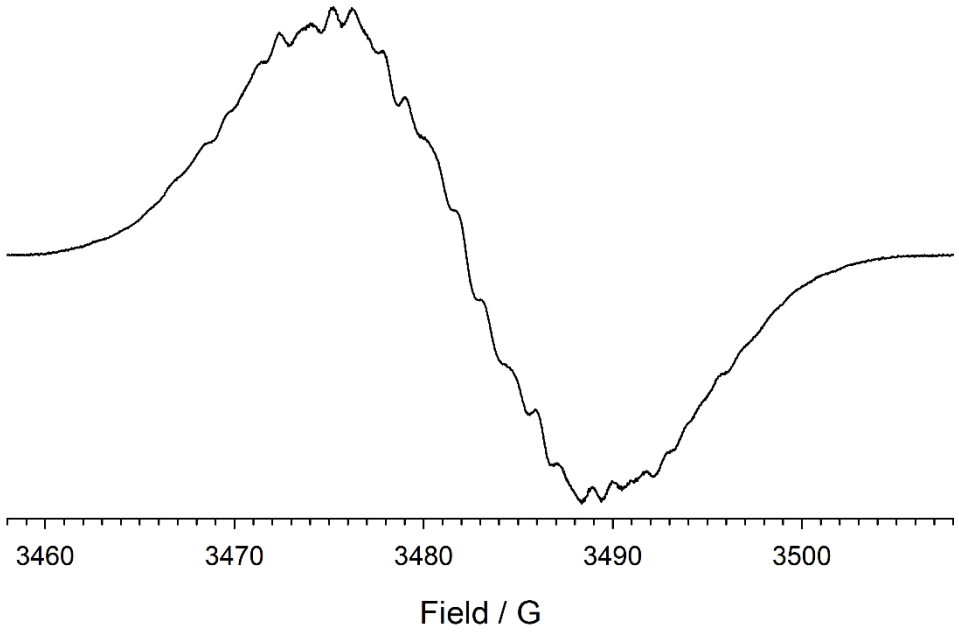

Figure S29. EPR spectrum of the radical cation **11**$^{+\bullet}$ in CH_2Cl_2.

References

[1] *DigiSim* 3.05; BioAnalytical Systems: West Lafayette, IN; www.bioanalytical.com.

[2] Bard, A. J.; Faulkner, L. R. *Electrochemical Methods. Fundamentals and Applications*; Wiley: New York, 1980. Chapter 6.

[3] R. S. Nicholson, R. S. *Anal. Chem.***1965**, *37*, 1351.